IJCTA, 10(02), 2017, pp. 205-215

Design of Dual-Bridge High Frequency Resonant DC/DC Converter for Storage Application

V. Thirumurugan* K. Senthilkumar* and S. Manoharan**

Abstract : A bidirectional dual-bridge high-frequency secluded resonant DC-DC converter is getting hold of more attention in renewable energy system due to its high power density, small size, reducing pressure and removal of electromagnetic interference noise. In this paper the simulation of dual bridge LC-L resonant converter is carried out for resistive and battery load. The simplified steady state analysis with complex ac analysis is specified and conditions for zero voltage switching are presented accordingly. A closed loop control operation of a converter using PI controller is recommended to reduce the reverse power flow for battery load.

Keywords : ZVS(zero voltage switching), DAB(dual active bridge), DC-DC converter, renewable energy sources.

1. INTRODUCTION

With the growing demand for electric power in future automobiles, telecom and computer systems, hybrid vehicle systems and aviation systems, people have identified the key importance of renewable energy sources to these systems [1]-[4]. The bidirectional dc-dc converter plays an vital role to interface between high voltage bus where energy generation device such as photovoltaic panel or other sources are installed, and a low voltage bus, where generally energy storage equipments such as a battery or super capacitor is coupled as shown in fig. 1. The input to this converter is normally variable dc voltage sources like photovoltaic, fuelcell or ac sources with mutually changing in magnitude and frequency. The output of this converter is dc that can be feed to dc load, energy storage device are fed to utility through an inverter. The power level of such type of converter is usually less than 100 kW [5]. A dual bridge converter (DBC) is normally consisting of two active bridges connected by high frequency transformer and power transfer inductor. The operating frequency of dual bridge converter(DBC) is very high which offers many advantages like light weight and smaller size of reactive components, power delivery with faster transient response [6]. Compared to traditional dc-dc converters, the bidirectional (DAB) have many advantages, like high reliability, electrical isolation, ease of soft switching control and bidirectional power flow.

The dual active bridge resonant converter is a arrangement of two active bridges with resonant tank as shown in fig. 2. Two active bridges are linked by a resonant tank and HF transformer. The resonant tank is either parallel resonant or series resonant or combination of both. It can be capacitor inductor, series combination of LC or parallel combination of LC. Zp is a parallel resonant tank which can be positioned on any side of the transformer. The series resonant converter has disadvantage of voltage regulation at light load while parallel resonant converter causes low efficiency at reduced load due to

* Assistant Professor, Department of Electrical and Electronics Engineering, The Kavery Engineering College, Tamilnadu

** Professor and Head, Department of Electronics and Instrumentation Engineering, Karpagam College of Engineering Tamilnadu, India

circulating current. Series-parallel LC-L resonant converters overcome largely of the limitations of series and parallel resonant converters. The leakage inductance and magnetizing of a HF transformer could be utilized as part of parallel resonant tank Zp and series resonant tank Zs respectively [7]. The power flow through the resonant tank can be maintained steadily by controlling phase shifts between the gating signals of the two bridges.

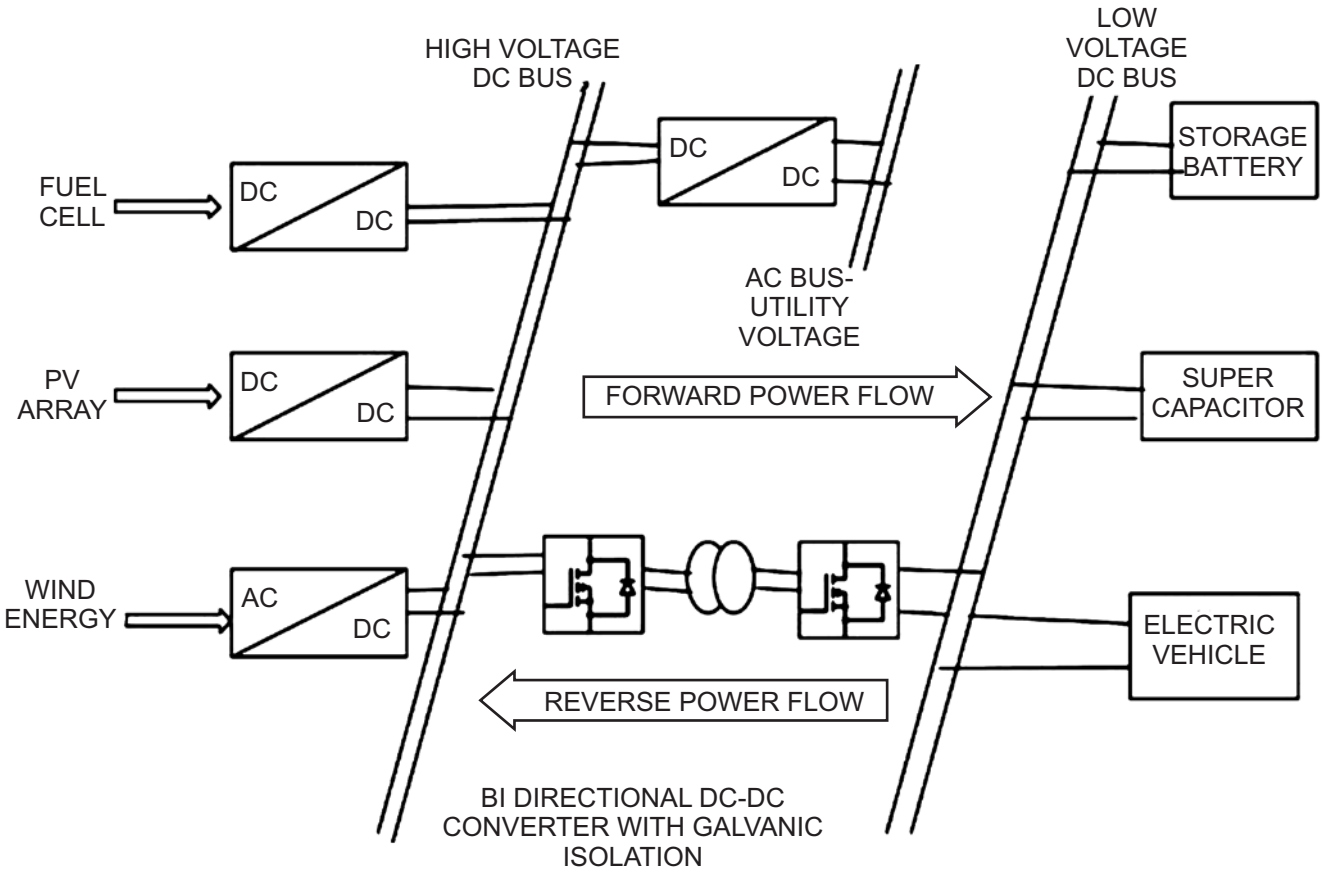

Figure 1: Typical application of secluded bidirectional dc-dc converter for power distribution in a micro grid

In this paper the near analysis using complex circuit analysis method is used to estimate the converter and conditions for ZVS is derived accordingly.

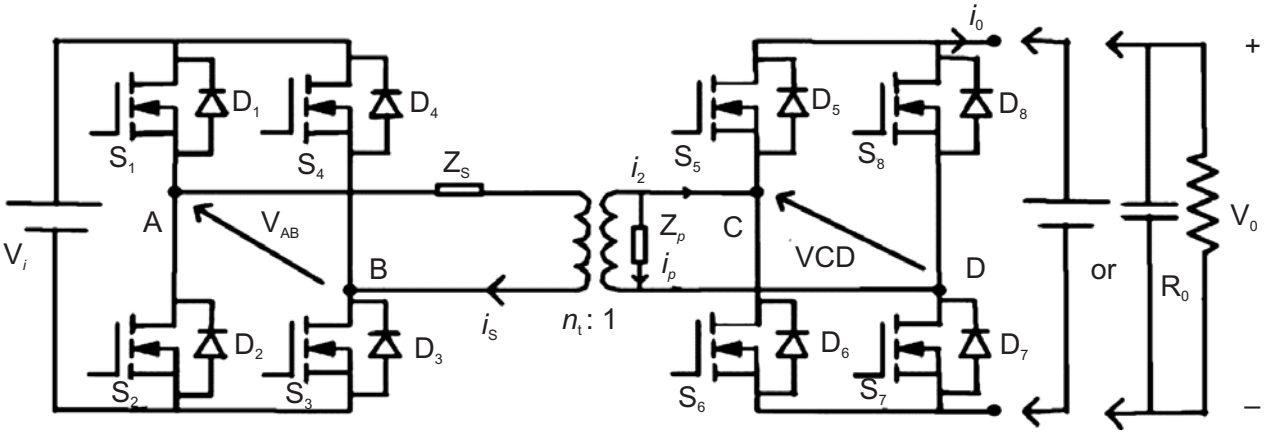

Figure 2: A dual-bridge converter with a generalized resonant tank

Simulation results for both battery load and resistive element are included for the purpose of validation. A suitable closed-loop control strategy has been used for battery load to minimize the reverse power flow.

2. MODIFIED COMPLEX AC ANALYSIS OF DUAL BRIDGE HIGH FREQUENCY RESONANT CONVERTER

In complex ac analysis approach, only primary component of voltages and currents are considered while all other harmonics are ignored. It is assumed that all switches, diodes and transformer are ideal [8] [10]. The leakage and magnetizing division of transformer are used as a part of series and parallel resonant tank by suitable arrangement. The outcome of snubber circuit is also ignored. All the parameters on secondary side of HF transformer have been taken to primary side and are denoted by superscript " ' ". The reactances of Z_P and Z_S are defined as X_P and X_S respectively. Two ac equivalent circuit analysis methods are specified for dc voltage source load and resistive load with capacitive filter, respectively. Both methods could be functional for either of the two types of load, because the load resistance can be regarded as the equivalent load resistance of a dc voltage source with the intended power at $P_0 = V_0^2/R_F$, $R_F' = n_t^2(V_0^2/P_0)$ where R_F is the primary side reflected equivalent full load resistance and n_t is transformer turns ratio. The equivalent circuit of converter in phasor domain can be drawn as shown in fig 3

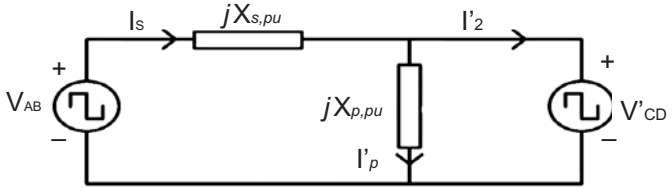

Figure 3: The equivalent circuit of the dual-bridge resonant converter with resonant tank

For handiness the base values are taken as bellow:

$$V_B = V_1 ; Z_B = R'_F ; I_B = V_B/Z_B \quad (1)$$

The regularized frequency F is given by;

$$F = \omega_s/\omega_r = f_s/f_r \quad (2)$$

Where $f_s = \omega_s/2\pi$ is switching frequency and $f_r = \omega_r/2\pi = 1/2\pi\sqrt{(LsCs)}$ is frequency of a resonant tank. The regularized values of all the reactances are specified by:

$$X_{s,pu} = X_s/Z_B \quad (3)$$

$$X_{p,pu} = X'_p/Z_B \quad (4)$$

Where X_s is a reactance of series resonant tank and $X'_p = n_t^2 X_p$ is a primary side reflected reactance of parallel resonant tank.

Since output voltage of secondary side converter V'_0 is asumed to be constant, the reflected converter input voltage V'_{CD} is a square wave through magnitude of V'_0. Thus the r.m.s value of fundamental input voltage V'_{CD} is given as:

$$V'_{CD,rms} = \frac{4}{\sqrt{2\pi}} V'_0 \quad (5)$$

The secondary bridge input current i'_2 is taken to be approximately sinusoidal. Due to active rectifier control, the rectifier input current i'_2 is supposed to lead the voltage V'_{CD} by phase shift angle $-\theta$ .Thus r.m.s value of secondary current is given by:

$$I'_{2\,rms} = \frac{\pi}{\sqrt{B}\cos\theta} I'_0 \quad (6)$$

Where I_0' is an average value of i_0'

Because of active rectifier, output current I_0' may go negative for small portion of each cycle, which means sometimes power is transferred from secondary side to primary side. Thus in case of conventional complex ac analysis it is pertinent to represent the whole secondary part with an equivalent impedance $Z_{ac} = Z_{ac} \angle -\theta$ instead of pure resistance.

The magnitude of equivalent ac impedance is got from

from equations (5) and (6).

$$Z_{ac} = \frac{V'_{CD\,rms}}{I'_{2\,rms}} = \frac{BV'_2\cos\theta}{\pi^2 I'_0} = \frac{BR'_0\cos\theta}{\pi^2} \quad (7)$$

The normalize ac impedance is given as :

$$Z_{ac,\,pu} = \frac{Z_{ac}}{R'_F} = \frac{BR'_0\cos\theta}{\pi^2 R'_F} = \frac{B\cos\theta}{\pi^2}H \quad (8)$$

Where R'_0 is an output load resistance while $H = R'_0 / R'_f$ is regularized load resistance and $H \in [1, \infty]$ as load goes on decreasing from full load to nil load.

By means of equivalent impedance, the converter equivalent circuit in phasor domain can be drawn as shown in fig. 4.

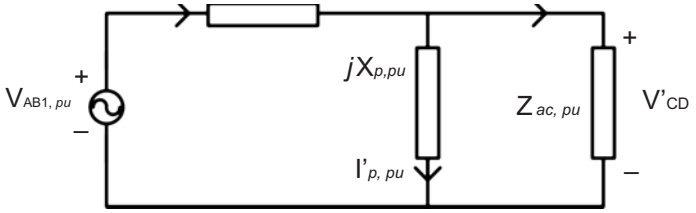

Figure 4: The dual-bridge resonant phasor domain equivalent circuit of converter with equivalent impedance

$V_{AB1,\,pu}$ and $V'_{CD1,\,pu}$ are the regularized fundamental phasor components of V_{AB} and V'_{CD} respectively. The expressions for regularized fundamental components of V'_{CD} and V_{AB} in phasor domain are:

$$V_{AB1,\,pu} = \frac{4}{\pi} e^{j\left(w_s t - \frac{\pi}{2}\right)} \quad (9)$$

$$V'_{CD1,\,pu} = \frac{4M}{\pi} e^{j\left(w_s t - \varnothing - \frac{\pi}{2}\right)} \quad (10)$$

Here ϕ is phase angle between primary side voltage $V_{AB1,\,pu}$ and secondary side voltage $V'_{CD1,\,pu}$ which is given by provided delay in gating signals of secondary converter with respect to gating signals of primary converter. M is the converter gain, given as:

$$M = \frac{V'_0}{V_i} \quad (11)$$

By applying principle of superposition, the three current phasors can be evaluated as:

$$I_{s,\,pu}(t) = \frac{4}{\pi X_{s,\,pu}}(Me^{-j\varnothing} - 1)e^{jw_s t} \quad (12)$$

$$I'_{2,\,pu}(t) = \frac{4}{\pi X_{s,\,pu}}[M(1+K)e^{-j\varnothing} - 1)]e^{jw_s t} \quad (13)$$

$$I'_{p,\,pu}(t) = -\frac{4M}{\pi X_{p,\,pu}} e^{-j(w_s t - \varnothing)} \quad (14)$$

where :

$$K = \frac{\omega_s L_s - (1/\omega_s C_s)}{\omega_s L_p} = \frac{L_s}{L_p}\left(1 - \frac{1}{F^2}\right) \quad (15)$$

Thus the resonant currents in time domain can be obtained as :

$$i_{s,\,pu}(t) = \frac{4[M\cos(\omega_s t - \varnothing) - \cos(w_s t)]}{\pi X_{s,\,pu}} \quad (16)$$

$$i'_{2s,\,pu}(t) = \frac{4[\mathrm{M}\cos(\omega_s t - \varnothing)(1+\mathrm{K}) - \cos(w_s t)]}{\pi \mathrm{X}_{s,\,pu}} \quad (17)$$

$$i_{p,\,pu}(t) = \frac{4\mathrm{M}\cos(\omega_s t - \varnothing)}{\pi \mathrm{X}_{p,\,pu}} \quad (19)$$

The soft switching condition for two bridges are :

$$i_{s,\,pu}(0) < 0 \text{ for the primary bridge, and} \quad (19)$$

$$i'_{2s,\,pu}\left(\frac{\varnothing}{\omega_s}\right) > 0 \text{ for the secondary bridge.} \quad (20)$$

From the equations (16) and (17) the conditions can be re-written as:

$$\frac{4[\mathrm{M}\cos(\varnothing) - 1]}{\pi \mathrm{X}_{s,\,pu}} < 0 \quad (21)$$

$$\frac{4[\mathrm{M}(1+\mathrm{K}) - \cos(\varnothing)]}{\pi \mathrm{X}_{s,\,pu}} > 0 \quad (22)$$

The solutions to realize zero voltage switching of two bridges are :

$$\cos\varnothing < \min\left[\frac{1}{\mathrm{M}}, \mathrm{M}(1+\mathrm{K})\right] \quad (23)$$

To gratify equation (23) it is better that both 1/M and M (1+ K) are greater than 1 since maximum value of cos ϕ is 1. For this M be supposed to be less than one so that the soft switching of primary bridge is possible and once M ≤ 1 soft switching of secondary bridge is possible by appropriately selecting the value of K.

Switch peak currents on primary and secondary sides of HF transformer are:

$$\mathrm{I}_{s,\,pu} = \frac{4\sqrt{\mathrm{M}^2 + 1 - 2\mathrm{M}\cos\varnothing}}{\pi|\mathrm{X}_{s,\,pu}|} \quad (24)$$

$$\mathrm{I}'_{2p,\,pu} = \frac{4\sqrt{(\mathrm{M}+\mathrm{MK})^2 + 1 - 2\mathrm{M}(1+\mathrm{K})\cos\varnothing}}{\pi|\mathrm{X}_{s,\,pu}|} \quad (25)$$

The converter gain M can alsobe given from fig. 4 as :

$$\mathrm{M} = \left|\frac{\mathrm{Z}_{ac,\,pu} \mid j\,\mathrm{X}_{p,\,pu}}{j\,\mathrm{X}_{s,\,pu} + \mathrm{Z}_{ac,\,pu} \mid j\,\mathrm{X}_{p,\,pu}}\right| = f(\theta) \quad (26)$$

From equation (26) it is finalized that M is a function of θ, which is the angle difference between $\mathrm{V'}_{\mathrm{CD1},\,pu}$ and $\mathrm{I}_{\mathrm{S.P.U}}$. Here θ is non-controllable parameter; hence M can be controlled by valuating another angle β, which is the difference between $\mathrm{V}_{\mathrm{AB1},\,pu}$ and $\mathrm{I'}_{\mathrm{2.P.U}}$, given as:

$$\theta = \varnothing - \beta \quad (27)$$

Where,

$$\beta = -\tan^{-}\left(\frac{(1+\mathrm{K})\mathrm{Z}_{ac,\,pu}\sin\theta}{(1+\mathrm{K})\mathrm{Z}_{ac,\,pu}\cos\theta - \mathrm{X}_{s,\,pu}}\right) \quad (28)$$

Hence from equations (26), (27) and (28) *M* can be written as

$$\mathrm{M} = \frac{8\mathrm{H}\sin\varnothing}{\pi^2\,\mathrm{X}_{s,\,pu}} \quad (29)$$

From above equation (29) it is accomplished that M is a function of ϕ, then M can be tuned by taking proper value of ϕ.

3. SIMULATION RESULTS

The simulation of dual-bridge LC-L resonant converter is carried out in Simulink for both resistive and battery load, and the analysis is done accordingly.

A. Simulation results for resistive load

The dual-bridge LC-L converter is assumed to work at the following conditions:

$$V_1 = 200V,$$
$$V_0 = 48V,$$
$$M = 0.94,$$
$$F = 1.09,$$
$$K = 0.3.$$
$$f_s = 100\ kHz.$$

The resonant tank components can be taken as:

$$L_S = 87.54\ \mu H,$$
$$C_S = 35nF,$$
$$L_P = 50.42\mu H$$

The capacitive filter connected at output side is given by:

$$C = \frac{1}{4\sqrt{3} f_s\ \gamma\ R_L} \tag{30}$$

The full load (200 W) and half load (100 W) operations are shown in fig. 5 and fig. 6 respectively. The ZVS operation is established from the time plot of switches vs current. The output current of secondary bridge is *io*, whose average value is output dc current. The negative part of *io* exists only for little portion of each cycle which indicates lower circulating current and higher efficiency. The current in parallel inductor which is placed on secondary side of HF transformer, only relies on output voltage and is independent on load level. Comparison between Simulated and calculated values of different parameters is specified in following Table.

Tabel 1

Comparison Between Simulated and Calculated Values of Parameters At V_i = 200V, V_0 = 48V and f_s = 100 kHz

Load Level	*Parameters*	*Simulated Value*	*Calculated Value*
Full Load 200W	M	0.9761	0.9792
	I_S	1.64A	1.45A
	I_2	6A	7.5A
	ϕ	3.6°	3.3°
Half Load 100W	M	0.9792	0.95
	I_S	0.84A	0.76A
	I_2	3.2A	3.16A
	ϕ	1.8°	1.6°

B. Simulation results for battery load

The simulation of LC-L resonant converter is performed in Simulink for various battery charging conditions. The ZVS is confirmed from simulation plots of fig. 7. While drawing simulations for battery load it is experimental that, as the battery charging goes on increasing the amount of reverse power flow from battery side to supply increases *i.e*. negative part of *io* keep on increasing. This leads to reduction in the efficiency of converter and high conversion losses which results in slower rate of battery charging. Here simulation results of LC-L converter for battery load at 90% of state of charging (SOC) are presented.

The converter works at following conditions:

$$V_1 = 200V;$$
$$V_2 = 50V;$$
$$\text{Battery} = 1.52Ah.\ 48V,$$
$$\varnothing = 1.5°$$

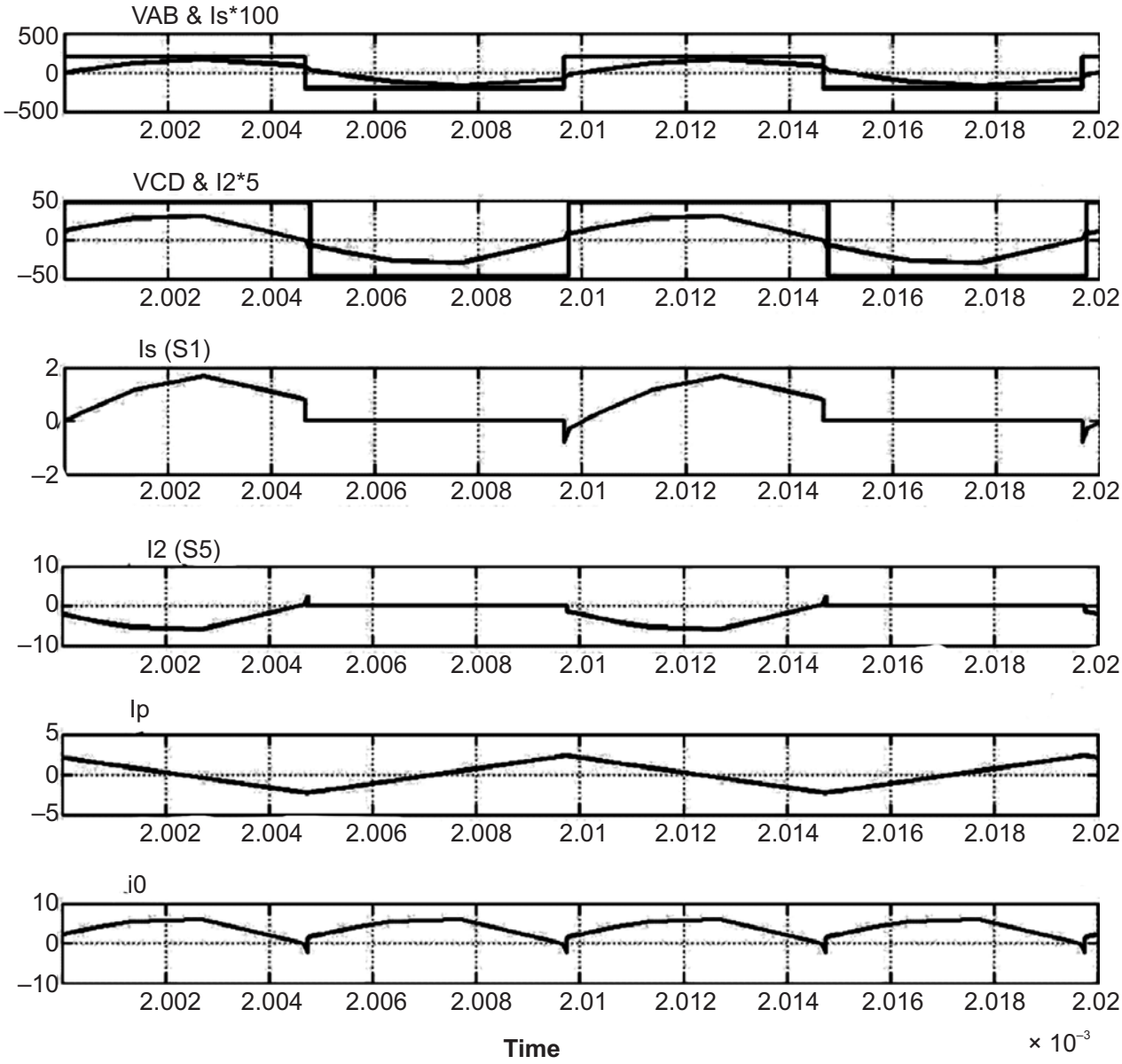

Figure 5: Results of a dual-bridge LC-L resonant converter at P_0 = 200 W, V_0 = 48 V for resistive load-Simulated

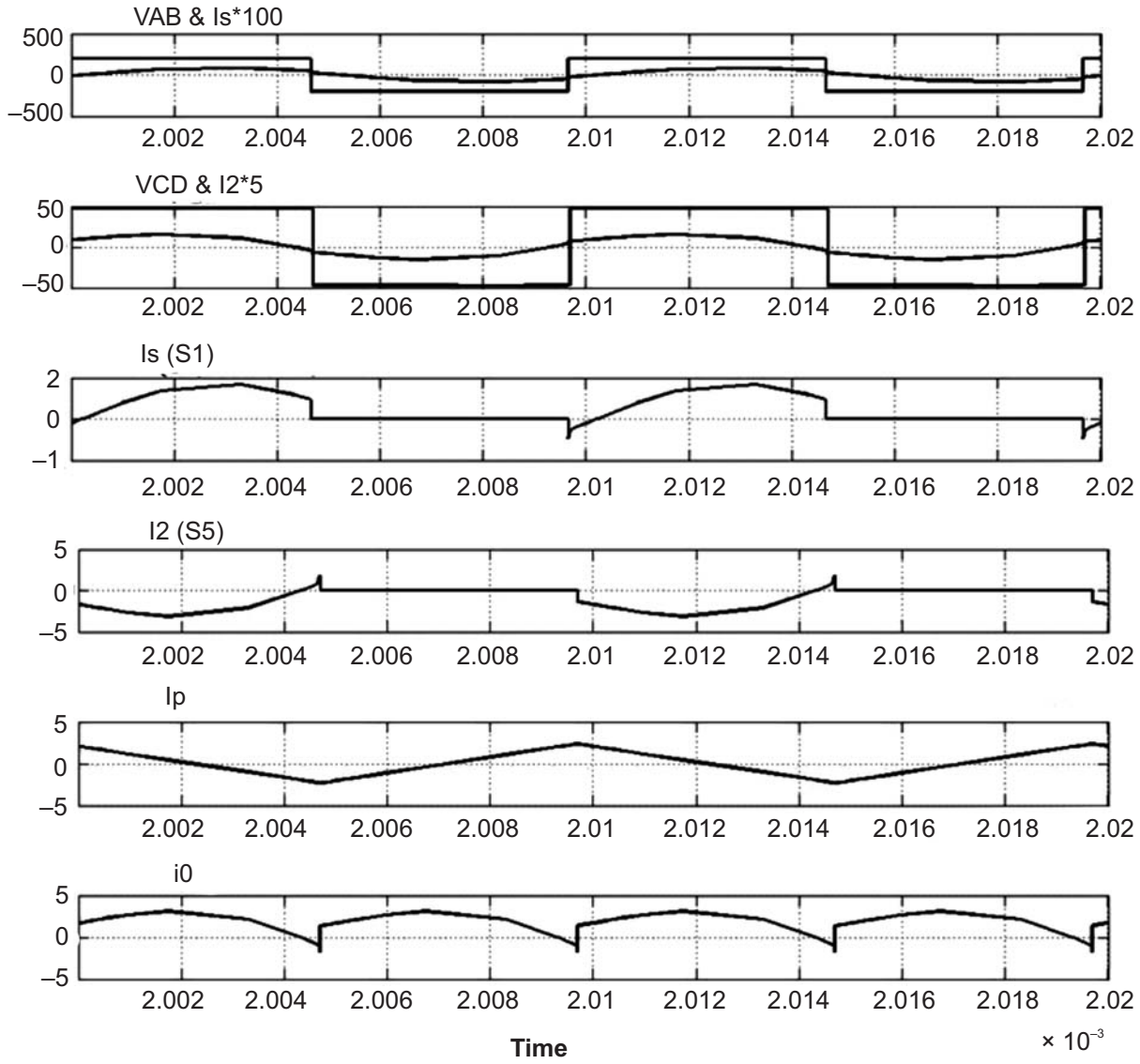

Figure 6: Simulation results of a dual-bridge LC-L resonant converter at P_0 = 100 W, V_0 = 48 V for resistive load

Comparison between calculated and simulated value of parameters is given in following Table 2.

Table 2

Comparison Between Simulated and Calculated Values of Parameters at V_i = 200V, V_0 = 50V AND f_S = 100kHz

SOC	*Parameters*	*Simulated*	*Calculated*
90%	M	0.98	0.95
	I_s	0.36A	0.5A
	I_2	2.5A	2.5A
	ϕ	1.8°	1.5°

Digital Control Scheme to avoid the Reverse Power Flow

It is here recommended that PI controller is used to prevent the reverse power flow. The arrangement of proportional and integral terms is important to raise the speed of the response and also to remove the steady state error. Fig.8 shows the closed loop control strategy to minimize the reverse power flow. Here the output current (Io) of converter is compared with the reference value and the error signal is given to PI controller with some gain in error signal.

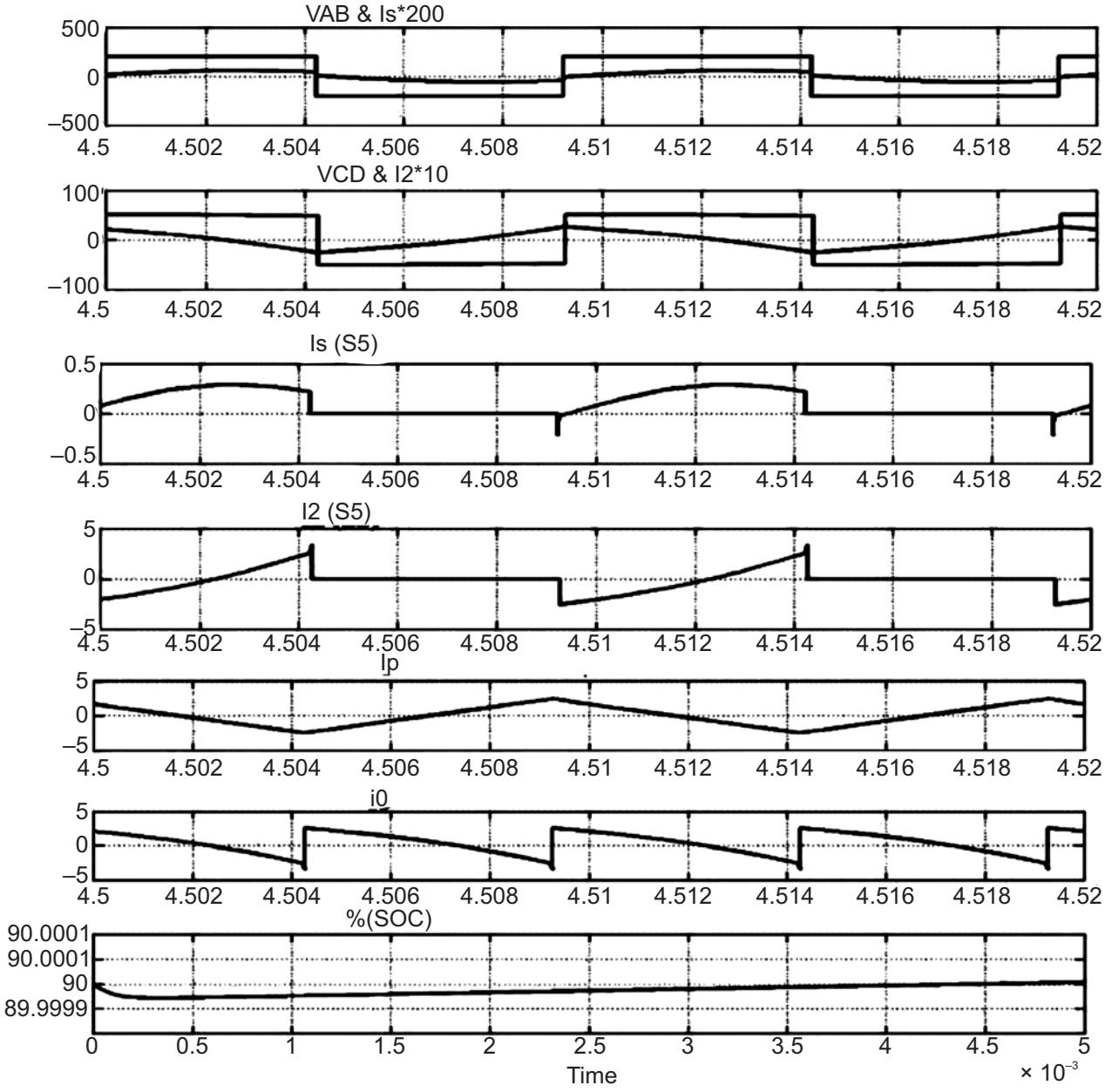

Figure 7: Results of LC-L Resonant converter for battery load without PI controller at 90% SOC- Simulated.

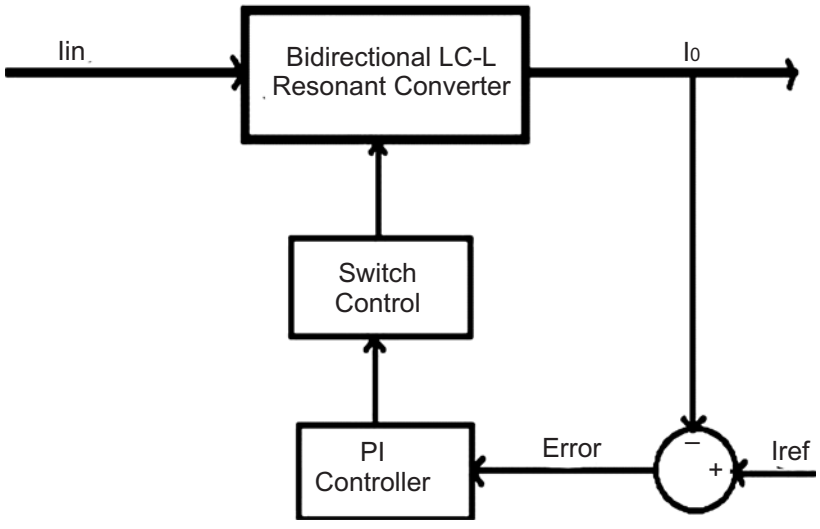

Figure 8: Closed-loop PI controller for high frequency LC-L resonant converter

The PI controller processes the error signal and produces the control signal which is given to the switch control block. The pulse frequency modulation block generates the frequency pulse according to control signal which retain unidirectional power flow.

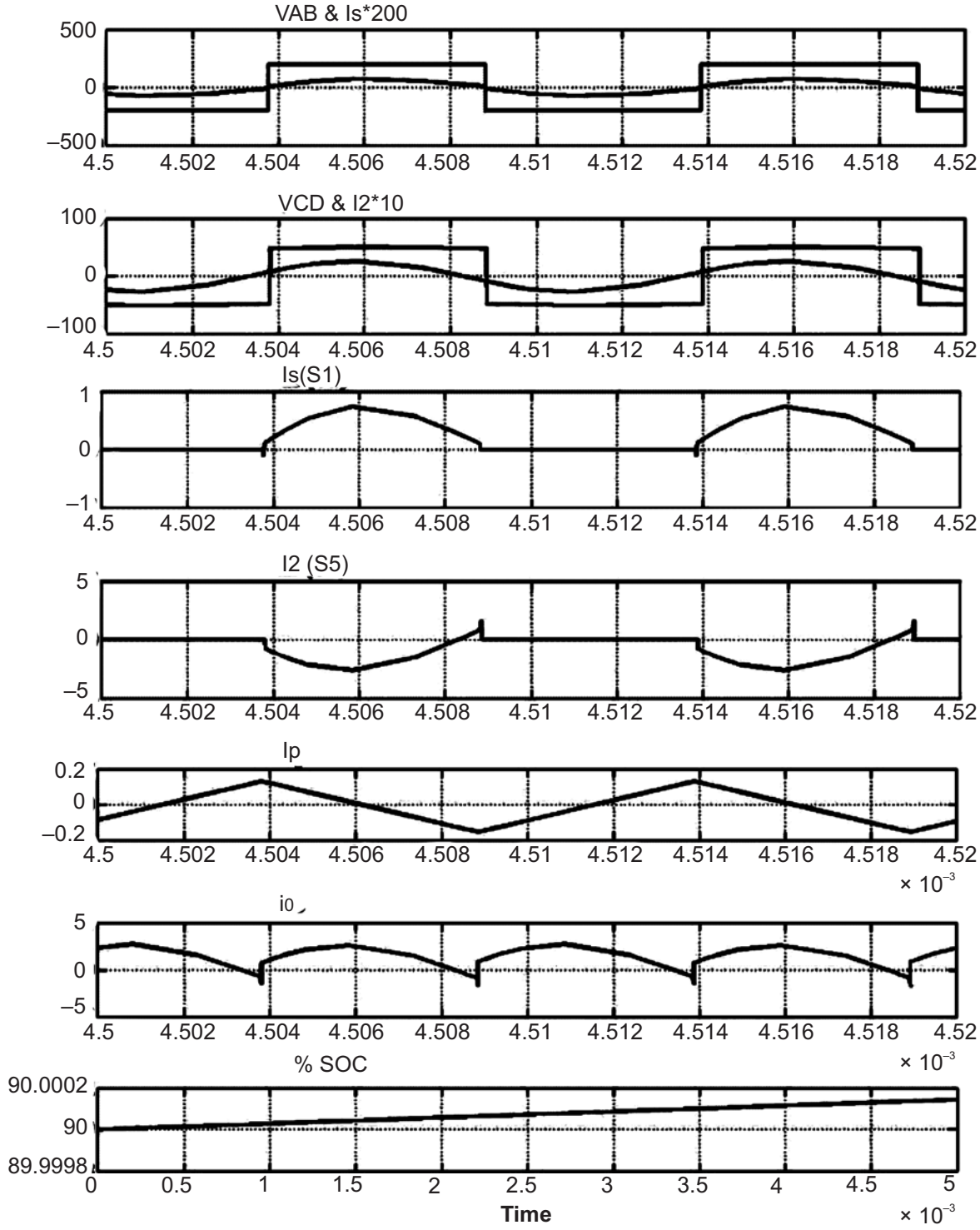

Figure 9: Simulation results of LC-L resonant converter for battery load with PI controller at 90% SOC

The control action of a proportional and integral controller is defined by following equation:

$$u(t) = K_p e(t) + K_i \int e(t)dt \quad (31)$$

Where $u(t)$ – is actuating signal

and $e(t)$ – is error signal.

– Proportional gain constant
– Integral gain constant.

The simulated result with battery load at 90% SOC using PI controller is shown in fig. 9.The converter works at following conditions:

$$V1 = 200V;$$
$$V2 = 50V;$$
$$\text{Battery} = 1.52Ah.$$
$$48V,\ M = 0.992,$$
$$\varnothing = 1.5^{\circ},$$
$$K_P = 1.9,$$
$$K_I = -0.3.$$

From fig. 9, it is observed that by using PI controller the reverse power flowing through converter decreases to large amount and thus it reduces the losses and increases the efficiency of a converter.

4. CONCLUSION

In this paper the analysis of dual bridge high frequency series parallel LC-L resonant converter is carried out with modified complex ac analysis approach and accordingly conditions for ZVS are derived for both the bridges. The simulation carried out in Simulink gives the detail view of all operational parameters. The simulation plot validates the theoretical analysis. From simulation it is observed that the ZVS is carried out in both converters. Closed loop control operation using PI controller is addressed for battery load which increases the converter efficiency by minimizing reverse power flow.

5. REFERENCES

1. Huang-Jen Chiu and Li-Wei Lin. “A bidirectional DC-DC converter for fuel cell electric vehicle driving system,” IEEE Transactions on Power Electronics, vol. 21, no. 4, pages: 950-958, 2006.
2. Dehong Xu, Chuanhong Zhao, and Haifeng Fan, “A PWM plus phase shift control bidirectional DC-DC converter,” IEEE Transactions on Power Electronics, vol. 19, no. 3, pages: 666-675, 2004.
3. R. W. De Doncker, D. M. Divan and M. H. Kheraluwala, “A three-Phase soft-Switched high power density DC/DC converter for high power applications,” IEEE Trans. Ind. Applicat., vol. 27, no. 1, pp. 63-73, Jan./Feb. 1991.
4. Xiaolong Shi, Jiuchun Jiang and Xintao Guo, “An Efficiency-Optimized Secluded Bidirectional DC-DC Converter with Extended Power Range for Energy Storage Systemsin Microgrids,” Energies 2013, 6, 27-44; doi:10.3390/en6010027.
5. X. D. Li and A. K. S. Bhat, “Analysis and Design of High-Frequency Secluded Dual-Bridge Series Resonant dc/dc Converter,” IEEE Trans. Power Electron., vol. 21, no. 2, pp. 850-862, April 2010.
6. Issa Batarseh, “Resonant converter topologies with three and four energy storage elements,” IEEE Trans. Power Electron., vol. 9, no.1, pp. 64-73, Jan. 1994.
7. Ashoka K. S. Bhat, “Analysis and Design of LCL-Type Series Resonant Converter,” IEEE Transactions on Industrial electronics, Vol. 41, No. 1, February 1994.
8. X. D. Li and Akshay Rathore, “A general study of soft Switching ranges of dual-bridge resonant converters using a modified complex AC analysis approach,” the 6th IEEE Conference on Industrial Electronics and Applications (ICIEA), pp: 316-321, June 21-23, Beijing, 2011.
9. Kojori H. A., Lavers J. D., and Dewan S. B., “Steady state analysis and design of an inductor-transformer resonant DC-DC converter,” IEEE Industry Appl. Soc. Conf. Rei., 1987, pp. 984-989.
10. Xiaodong Li, Hong-Yu Li, Gao-Yuan Hu and Yu Xue, “A Bidirectional Dual – Bridge High - Frequency Secluded Resonant DC/DC Converter,”
11. Industrial Electronics and Applications (ICIEA), 8th IEEE Conference. pp. 49 – 54, 19-21, June 2013.